Supporting Information

Operation and Optimization of Microwave-heated Continuous Flow Microfluidics

Tai-Ying Chen[a], Montgomery Baker-Fales[a], and Dionisios G. Vlachos[a,b,*]

[a]Department of Chemical and Biomolecular Engineering, University of Delaware, 150 Academy Street, Newark, Delaware 19716, United States

[b]Catalysis Center for Energy Innovation, 221 Academy Street, Newark, Delaware 19716, United States

[*]Corresponding author; vlachos@udel.edu (D.G. Vlachos)

Description of Attenuator Arrangement

Temperature is measured at the junction of the bend and of the second 'leg' of the U-shaped microchannel as indicated in Scheme S2. This location was chosen for two primary reasons - firstly that the simulated temperature profile shows negligible sensitivity to small changes in axial position at this location in built U1 and U2 microchannels. Secondly, the location is within the field of view of the cavity's optical camera, which aids in keeping the fiber in position.

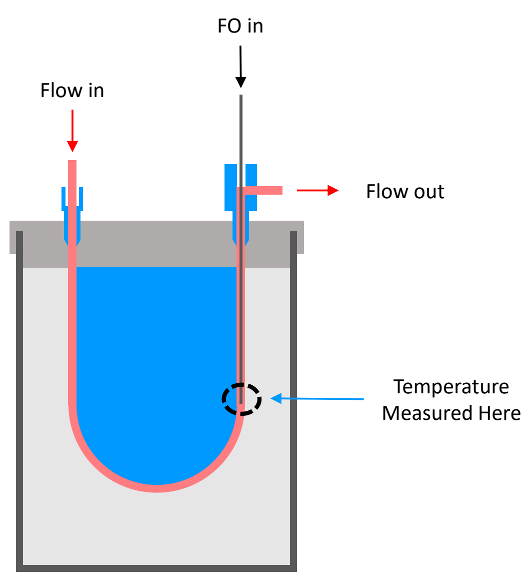

Scheme S1. Description of Attenuator and Optical Fiber Arrangement.

Demonstration of Steady State Temperatures

Temperature is measured in real time as microwave irradiation is applied to the cavity. These temperatures are logged to create a temperature-time profile. From the start of microwave irradiation, stream temperatures increase steadily. After 10-30 seconds of microwave irradiation, temperatures approach more stable values. Based upon this, a time of 90 seconds of microwave irradiation was chosen as the earliest approximation to steady state. Simulations show similar behavior. Typical temperature-time profiles are offered in Figure S1.

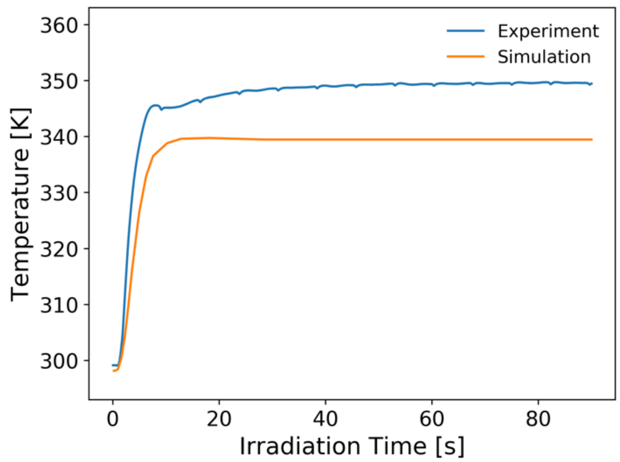

Figure S1. Time under irradiation stream temperatures using the U2 microchannel (ID = 0.762 mm) with input power = 40 W and flow rate = 0.8 mL/min.

Dielectric Properties of Water and 20 wt% NaCl Solution

Table S1. Dielectric properties of water at 2.45 GHz. Reprinted from ref. 1 Copyright (2012), with permission from Elsevier.

Temperature [°C]	Relative complex permittivity [-]
20	78.0-10.5j
30	75.0-8.6j
40	72.0-6.7j
50	69.0-5.1j
60	66.2-3.85j
70	63.9-3.3j
80	62.7-3.1j
90	62.3-3.0j
100	62.0-2.9j

Table S2. Dielectric properties of 20 wt% NaCl solution at 2.45 GHz.[2]

Temperature [°C]	Relative complex permittivity [-]
20	78.05-28.82j
30	74.92-18.84j
40	71.67-15.13j
50	68.55-11.76j
60	65.17-9.09j
70	61.79-7.25j
80	58.41-5.59j
90	55.15-5.12j

Mesh Convergence Analysis

In *Physics-controlled Mesh setting* in COMSOL, the mesh for the U-shaped microchannel is set to "Finer", where the element sizes are between 0.000217 and 0.00201 [m]; the mesh for PFA channel wall is set to "Fine", where element sizes are range from 0.00212 to 0.017 [m]; and the mesh for the rest of the simulation domains are set to "Normal", where element sizes range from 0.00381 to 0.0212 [m]. Different element sizes are employed to carry out mesh independence analysis. The maximum/minimum element sizes employed for the U-shaped microchannel are 0.00603/0.0007, 0.00402/0.000435, 0.00201/0.000217 and 0.00101/0.000109 [m], respectively. The mesh is automatically created and adapted by COMSOL, with the defined element size. Element sizes are selected when further mesh refinement changes both the averaged power dissipation density and the outlet temperature by less than 1%. Therefore, considering the computational cost, a 0.00201/0.000217 of maximum/minimum element size is chosen. A single simulation takes at least an hour computational time using 4 CPUs.

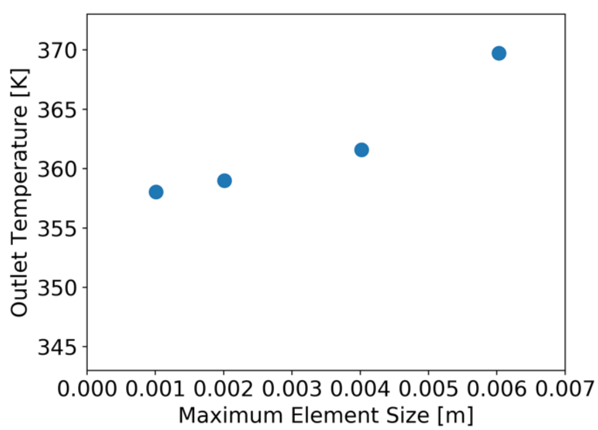

Figure S2. Outlet temperature with respect to different element sizes.

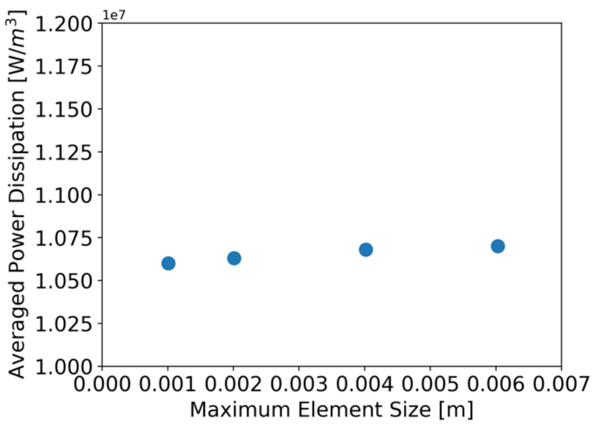

Figure S3. Averaged power dissipation density with respect to different element sizes.

Combinations of Variables used in Performing CFD Simulations

Table S3. Combinations of variables used in performing CFD simulations and building the GBRT model.

Variable	Value
Internal diameter, ID	1, 1.5, 2, 2.5, 3, 3.5, 4, 4.5, 5, 6, 7, 8 mm
Distance of the microchannel from cavity bottom, p	5, 20, 35, 40, 45 mm
Distance between legs, D	5, 25, 30 mm
Superficial velocity	0.00822, 0.01644, 0.0411 m/s
Input power	50 and 100 W

Hyperparameters of Gradient Boosting Regression Tree

The hyperparameters tuned in this work are the maximum tree depth, the number of trees, and the learning rate. The hyperparameters' selection is based on 4-fold cross-validation results. The maximum depth of the tree is selected as 7; the number of trees is set as 100; and the learning rate is set as 0.1.

Bayesian Optimization

In Bayesian optimization, a gaussian process (GP) is determined from a mean function (the average of all functions) and a covariance kernel function, which specifies the form of the individual functions and how they differ from the mean function. The GP is used to make predictions at unobserved points and propose the next sampling points. A typical Bayesian optimization procedure starts with finding the next sampling point by optimizing the acquisition function over the GP. Once a new observation is obtained from *f*, it is added to the previous observations and the GP is updated. The process is repeated 100 times to obtain the optimal. In this work, we use the typical Matern covariance function, Eq. (S1), as the kernel function,

$$C_\nu(\mathrm{d}) = \sigma^2 \frac{2^{1-\nu}}{\Gamma(\nu)} (\sqrt{2}\nu \frac{d}{\rho})^\nu K_\nu(\sqrt{2}\nu \frac{d}{\rho}) \tag{S1}$$

where d is the distance between two points, σ is the standard deviation, ν and ρ are non-negative parameters, Γ represents the gamma function, and K_ν is the modified Bessel function. In this work, ν equals to 1.5; and ρ is set as 1. The expected improvement, Eq. (S2), is chosen as the aquisition function

$$\mathrm{EI(x)} = \mathbb{E}[\max(f(x) - f^*),0] \tag{S2}$$

where f^* is the current best observation. This Bayesian optimization procedure used in this work is implemented using BoTorch[3], a open-source package in Python.

Demonstration of Single Tree Structure in Gradient Boosting Regression Tree

Since the gradient boosting regression tree is an ensemble method that combines the predictions from many basic decision tree estimators, the 100th tree in the model is shown in Figure S4 to demonstrate the tree structure.

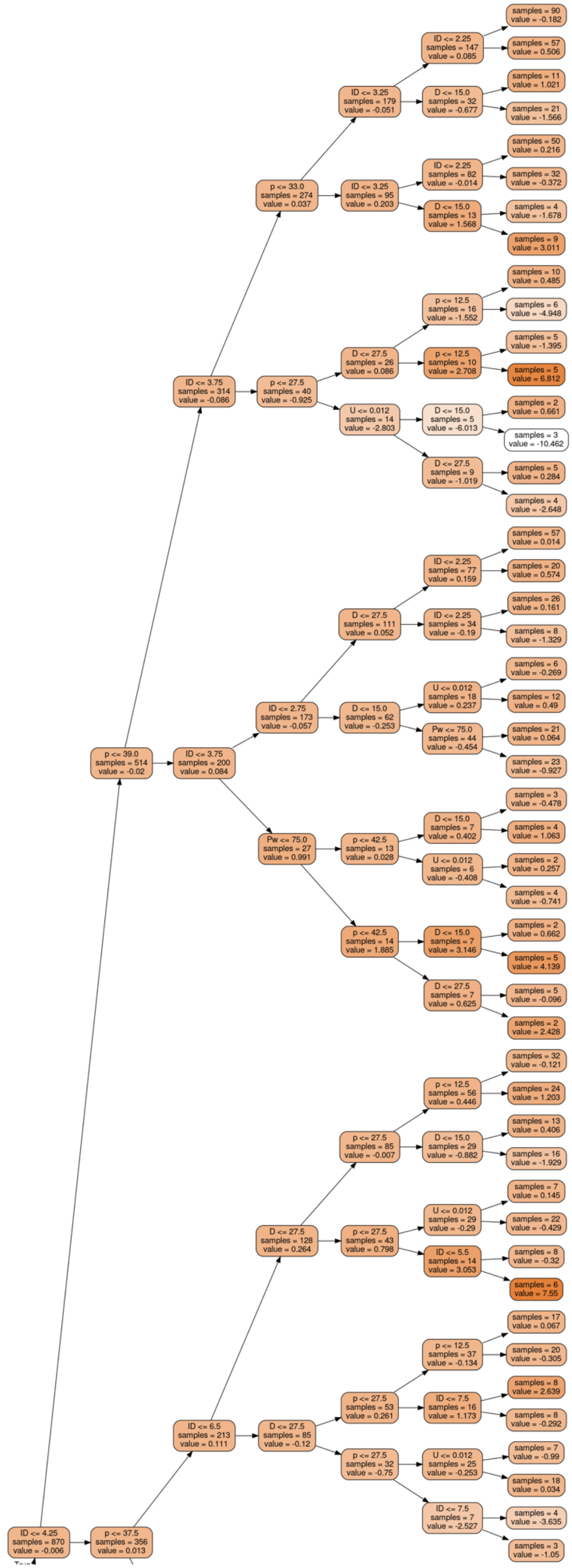

ID <= 4.25 samples = 870 value = -0.006
p <= 39.0 samples = 514 value = -0.02
ID <= 3.75 samples = 314 value = -0.086
p <= 33.0 samples = 274 value = 0.037
ID <= 3.25 samples = 179 value = -0.051
ID <= 2.25 samples = 147 value = 0.085
samples = 90 value = -0.182
samples = 57 value = 0.506
D <= 15.0 samples = 32 value = -0.677
samples = 11 value = 1.021
samples = 21 value = -1.566
ID <= 3.25 samples = 95 value = 0.203
ID <= 2.25 samples = 82 value = -0.014
samples = 50 value = 0.216
samples = 32 value = -0.372
D <= 15.0 samples = 13 value = 1.568
samples = 4 value = -1.678
samples = 9 value = 3.011
p <= 27.5 samples = 40 value = -0.925
D <= 27.5 samples = 26 value = 0.086
p <= 12.5 samples = 16 value = -1.552
samples = 10 value = 0.485
samples = 6 value = -4.948
p <= 12.5 samples = 10 value = 2.708
samples = 5 value = -1.395
samples = 5 value = 6.812
U <= 0.012 samples = 14 value = -2.803
D <= 15.0 samples = 5 value = -6.013
samples = 2 value = 0.661
samples = 3 value = -10.462
D <= 27.5 samples = 9 value = -1.019
samples = 5 value = 0.284
samples = 4 value = -2.648
ID <= 3.75 samples = 200 value = 0.084
ID <= 2.75 samples = 173 value = -0.057
D <= 27.5 samples = 111 value = 0.052
ID <= 2.25 samples = 77 value = 0.159
samples = 57 value = 0.014
samples = 20 value = 0.574
ID <= 2.25 samples = 34 value = -0.19
samples = 26 value = 0.161
samples = 8 value = -1.329
D <= 15.0 samples = 62 value = -0.253
U <= 0.012 samples = 18 value = 0.237
samples = 6 value = -0.269
samples = 12 value = 0.49
Pw <= 75.0 samples = 44 value = -0.454
samples = 21 value = 0.064
samples = 23 value = -0.927
Pw <= 75.0 samples = 27 value = 0.991
p <= 42.5 samples = 13 value = 0.028
D <= 15.0 samples = 7 value = 0.402
samples = 3 value = -0.478
samples = 4 value = 1.063
U <= 0.012 samples = 6 value = -0.408
samples = 2 value = 0.257
samples = 4 value = -0.741
p <= 42.5 samples = 14 value = 1.885
D <= 15.0 samples = 7 value = 3.146
samples = 2 value = 0.662
samples = 5 value = 4.139
D <= 27.5 samples = 7 value = 0.625
samples = 5 value = -0.096
samples = 2 value = 2.428
p <= 37.5 samples = 356 value = 0.013
ID <= 6.5 samples = 213 value = 0.111
D <= 27.5 samples = 128 value = 0.264
p <= 27.5 samples = 85 value = -0.007
p <= 12.5 samples = 56 value = 0.446
samples = 32 value = -0.121
samples = 24 value = 1.203
D <= 15.0 samples = 29 value = -0.882
samples = 13 value = 0.406
samples = 16 value = -1.929
p <= 27.5 samples = 43 value = 0.798
U <= 0.012 samples = 29 value = -0.29
samples = 7 value = 0.145
samples = 22 value = -0.429
ID <= 5.5 samples = 14 value = 3.053
samples = 8 value = -0.32
samples = 6 value = 7.55
D <= 27.5 samples = 85 value = -0.12
p <= 27.5 samples = 53 value = 0.261
p <= 12.5 samples = 37 value = -0.134
samples = 17 value = 0.067
samples = 20 value = -0.305
ID <= 7.5 samples = 16 value = 1.173
samples = 8 value = 2.639
samples = 8 value = -0.292
p <= 27.5 samples = 32 value = -0.75
U <= 0.012 samples = 25 value = -0.253
samples = 7 value = -0.99
samples = 18 value = 0.034
ID <= 7.5 samples = 7 value = -2.527
samples = 4 value = -3.635
samples = 3 value = -1.05

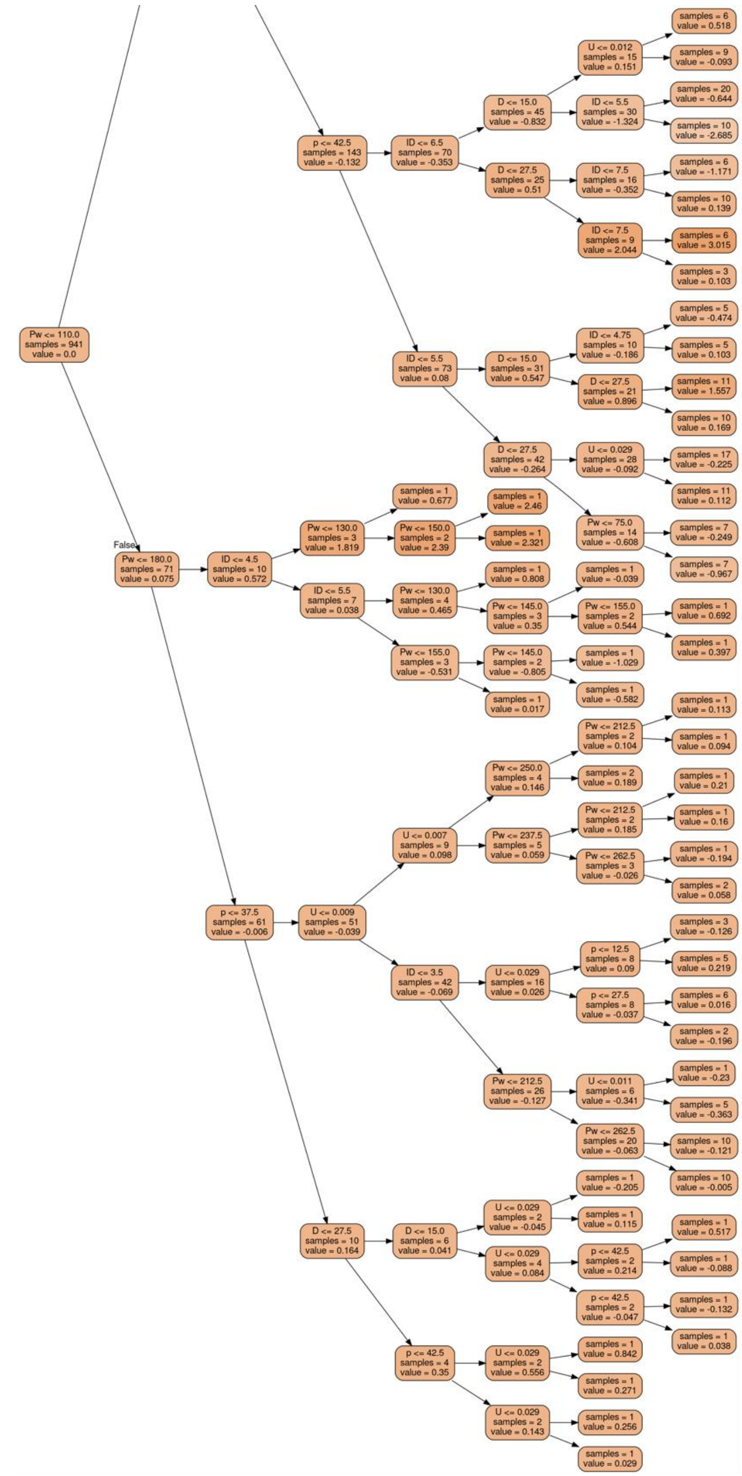

Figure S4. Demonstration of a single tree structure in gradient boosting regression tree.

References

1. Sturm, G. S. J.; Verweij, M. D.; van Gerven, T.; Stankiewicz, A. I.; Stefanidis, G. D., On the effect of resonant microwave fields on temperature distribution in time and space. *International Journal of Heat and Mass Transfer* **2012,** *55* (13), 3800-3811.
2. Kumar, A., Complex permittivity and microwave heating of pure water, tap water and salt solution. *International Journal of Electronics* **1979,** *47* (6), 531-536.
3. Balandat, M.; Karrer, B.; Jiang, D. R.; Daulton, S.; Letham, B.; Wilson, A. G.; Bakshy, E., BoTorch: Programmable Bayesian Optimization in PyTorch. *arXiv preprint arXiv:1910.06403* **2019**.